Topology Graph Pruning for Optical Mapping Methods using Edge Betweenness Centrality

Armagan Elibol[1] and Nak-Young Chong[1]

***Abstract*— Optical mapping is one of the most widely used application areas of low-cost robotic platforms. These platforms are in favor as they are relatively easy to use, to operate and to maintain. Acquired optical data (in the form of video and/or image) are valuable sources of information for both online (e.g., navigation, localization, mapping, and others) and offline processes (scientific interpretations, change detection, mapping, and others). The amount of data acquired has been continuously growing thanks to the emerging capabilities of mobile platforms in terms of autonomy allowing longer surveying time. This increases the need for fast and efficient methods to process the obtained data. Creating optical 2D maps from acquired data is composed of mainly image matching, trajectory estimation (Global Alignment (GA)) and image blending steps. In this paper, we discuss the usage of Edge Betweenness Centrality (EBC) concept to reduce the total number of overlapping image pairs to be used in the GA step. EBC allows selecting the image pairs that play a relatively key role in the topology graph. We also discuss the usage of graph energy as a decision criterion during image mosaicing iterations. We present experiments with several datasets to show the performance of the proposed method.**

I. INTRODUCTION

Low-cost mobile platforms with a limited sensor suite have been widely used for mapping purposes in different science disciplines (*e.g.*, geology, marine science, and many others). Visual maps can be created both online during the surveying mission and/or offline after obtaining the data. While maps being created through online processing provide valuable feedback for executing smooth operation (*e.g.*, in terms of navigation, coverage, and others), maps produced by offline processing provides better accuracy for further scientific analysis. Creating 2D maps from the images is known as image mosaicing problem [1]. Methods are generally aiming at inferring the topology (where images are denoted as nodes and overlapping image pairs are represented as edges between nodes) of the surveyed area [2]. When there is no positioning sensor information, images are the only source of information. Mostly, Feature-based image registration (or matching) methods have been commonly used to find a transformation between two images. This matching provides constraints on the image position. Once the edges are identified using image registration, GA methods are used to obtain the trajectory [3]. This is usually done through a (non-)linear minimization of a predefined error metric on identified feature point positions on images. Although there are some specially designed methods [4], [5], this minimization generally has a high computational cost (thus requires more time) due to the iterative nature of minimization and problem size. More recent studies have discussed and showed that eliminating some of the identified edges in the GA step would not corrupt the final quality of the obtained maps (mosaics) [6]. Image mosaicing frameworks generally work in an iterative manner of image matching attempts and trajectory estimation steps. Generating possible overlapping image pairs and selecting pairs to be matched are the two main processes of the image matching step. Especially, for the selection part, there are some studies using information theory [7], graph theory [6], visual similarity [8]. Information theory based methods require the propagation and maintenance of the covariance matrix of the estimated trajectory parameters and some further computations for ranking possible edges using (observation) mutual information. This brings some additional computational burden. Visual vocabularies are efficient for especially man-made structures and they require some initial training (vocabulary building step). Visual stopping criterion based on color invariant histograms was also proposed in [9] to stop iterations of searching for new overlapping image pairs, image matching, and trajectory estimation steps. However, it is not applicable to the cases of gray-scale images and if certain misalignment continues over iterations, this would not be inferred through the method as the color invariant histograms of intermediate mosaics would not be changed. This paper builds upon the methods proposed in [10], [6]. Instead of using information theory, we propose to use the graph energy concept as an overall measurement over iterations. This removes the necessity of a covariance matrix of the motion parameters and computing mutual information of possible edges. In order to select a subset of possible overlapping image pairs, we propose to use EBC as a part of the ranking score. These improvements reduce the overall computational cost. We present experimental evaluations for both online and offline mosaicing process with several datasets with different characteristics. In the following section, we explain our proposal of edge pruning based on EBC along with graph energy concept. In Section III, we present the experimental results with seven different datasets of underwater images. We draw our conclusions and underline some future works in the last section.

II. EDGE PRUNING USING EDGE BETWEENNESS CENTRALITY (EBC)

The graph G is composed of nodes (vertices) and edges (links) between nodes. A graph with n nodes can be rep-

[1]Authors are with the School of Information Science, Japan Advanced Institute of Science and Technology (JAIST), Ishikawa, Japan {aelibol,nakyoung}@jaist.ac.jp

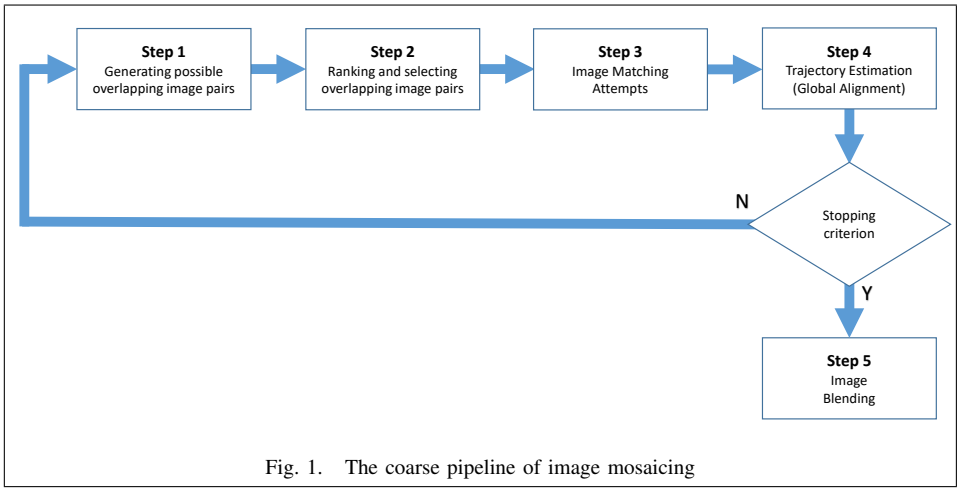

Fig. 1. The coarse pipeline of image mosaicing

resented by an adjacency matrix A of $n \times n$ with non-zero entries denoting edges between nodes. In our domain, images are represented as nodes and having an overlapping area between images are denoted as edges connecting nodes [2]. The coarse pipeline of creating image mosaics is given in Fig. I. In Step 1, the current available trajectory estimate is used to predict the overlapping image pairs by computing the distance between image centers. In Step 2, a graph adjacency matrix **A** is formed using both the existing edges that were successfully identified (or matched) in the previous iteration cycle and the possible edges predicted in Step 1. EBC values are then computed [11]. EBC value of an edge is the amount of a total number of shortest paths that pass through that edge [12]. It was proposed to be used for detecting communities in large graphs. Edges with higher values mean that they are in a more pivotal/bridge role in the graph and their removal from the graph might cause the graph to become disconnected. In order to rank the possible edges, we combine two scores, EBC values and approximate overlap percentage, in a weighted sum as in Eq. 1. The weights here are used as a balancing factor of selecting loop-closure pairs as well as having a high probability of being successfully matched as a result of image matching attempts.

$$f_s(i,j) = w_1 \cdot f_1(i,j) + w_2 \cdot f_2(i,j) \tag{1}$$

where $f_1(i,j)$ is the predicted overlap percentage and $f_2(i,j)$ is the EBC value between images i and j while w_1 and w_2 are weights with $w_1 + w_2 = 1$. After ranking the possible overlapping image pairs list, a subset of the list is selected instead of trying to match all of them as this would not be feasible computationally especially considering the size of the list during the first couple of iterations. This selection is done in a way to include all images as possible as it can. The main reasoning behind is to be able to update the whole trajectory estimate in Step 5 by adding new edges from all images. Our selection algorithm is motivated by the well-known concept of Non-Maximum Suppression (NMS) [13]. Our algorithm starts scanning the ranked list and picks an edge with the maximum score and allow to pick one more edge within its neighborhood. At the end of the selection, the same node would appear in a maximum of two edges. We use this way of selecting as it prevents including edges that belong to a certain part of the robot trajectory. The NMS based selection provides selecting image pairs throughout the whole trajectory. Afterward, the selected image pair list is passed to the next step of image matching. The images are attempted to be matched by using feature-based image registration and the trajectory is estimated by minimizing the pre-defined error metric on feature positions. The last but key step is the decision making step whether to continue for a new iteration or to stop. In this step, we propose to use the graph energy [14], which is defined as the sum of absolute values of eigenvalues of the adjacency matrix as given in Eq. 2.

$$E(A) = \sum_{i=1}^{n} |\lambda_i| \tag{2}$$

where A is the adjacency matrix of a graph with n nodes and $\lambda_i, (i = 1, 2, \ldots, n)$ is the eigenvalues of the adjacency matrix. Over iterations the change on the graph energy is monitored in relative manner using the Eq. 3.

$$\Delta(E)_t = \frac{E_{t+1} - E_t}{E_t} \tag{3}$$

where t and $t+1$ denotes iteration cycles. If this change is below a certain threshold in a small number (*e.g.,* two or three) of consecutive iteration cycles, the iteration cycle is stopped.

III. Experimental Results

We tested the performance of removing edges using EBC values with different real datasets. Scale Invariant Feature Transform (SIFT) [15] was used for detecting and describing distinctive points in images and Random Sample Consensus (RANSAC) [16] for outlier rejection and motion computation. The motion parameters were modeled as similarity transformations with 4 Degree of Freedoms (DOFs) namely, scale s, rotation θ, and translations tx and ty.

$$\mathbf{H} = \begin{bmatrix} s\cos\theta & -s\sin\theta & tx \\ s\sin\theta & s\cos\theta & ty \\ 0 & 0 & 1 \end{bmatrix}$$

and the first image frame was chosen as a global frame and its transformation was fixed to identity mapping. The trajectory estimation was done by minimizing the symmetric transfer error given in Eq. 4:

$$\min_{{}^1\mathbf{H}_2,{}^1\mathbf{H}_3,\ldots,{}^1\mathbf{H}_{N_{img}}} \sum_k \sum_s \sum_{j=1}^{c} \big(\parallel {}^k\mathbf{p}_j - {}^1\mathbf{H}_k^{-1} \cdot {}^1\mathbf{H}_s \cdot {}^s\mathbf{p}_j \parallel_2 + \parallel {}^s\mathbf{p}_j - {}^1\mathbf{H}_s^{-1} \cdot {}^1\mathbf{H}_k \cdot {}^k\mathbf{p}_j \parallel_2 \big) \quad (4)$$

where k and s are the successfully matched image indices, c indicates the total number of correspondences between the overlapping image pairs, N_{img} is the total number of images and $\mathbf{p} = (x, y, 1)^T$ denotes the coordinates of the points in the given image frame, expressed in homogenous coordinates.

First, we present some simulations for monitoring the change in graph energy as it is expected to behave similarly to the information measure used in [10]. Each new observation (regardless of how noisy it is) reduces the uncertainty of the system and this results in increasing the total amount of information since the information matrix is defined as the inverse of the covariance matrix of the variables. This theory allows concluding that each newly established edge in the topology graph decreases the uncertainty thus increases the total amount of information. This means that over the iteration cycles in Fig. I the total amount of information increases. Step 5 Stopping criterion was defined on monitoring the change on the total amount of information in [10]. Although there are some theoretical studies on the bounds of graph energy [17], we randomly generated adjacency matrices and compute their energy. The total amount of overlapping pairs and the energy computed are given in Fig 2. From the figure, graph energy grows smoothly with respect to the total number of edges in the graph. This behavior of graph energy is similar to the one with information theory. For

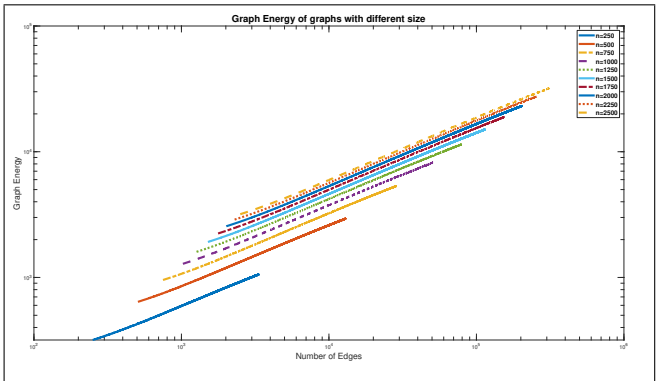

Fig. 2. Graph energy change over the total number of edges with different graph size plotted in log-scale. Energy increases with the number of edges. We generate $10,000$ random adjacency matrices with again random number of edges for each different size of graph ranging from 250 to 2500. For each graph size, the edges between consecutive nodes were existed in the every random matrix. We limit the maximum total number of edges to the $\%10$ of total number of possible edges $((n) \times (n-1)/2)$.

experiments, we used seven different datasets. The dataset properties are summarized in table I. The column *Ratio* is the ratio of existing overlapping image pairs identified using all-against-all image matching with respect to the all possible overlapping image pairs. This ratio provides insights about the density of the dataset. All datasets except Dataset IV and VI are from underwater medium and obtained by using underwater robots carrying a down-looking camera. Dataset IV was obtained through a down-looking camera carrying moving platform simulating a Unmanned Aerial Vehicle (UAV) while images of Dataset VI were cropped from a high-resolution image simulating real robot trajectory. To initialize the trajectory estimate, we assumed time-consecutive images have an overlap and they were matched to obtain initial trajectory estimate. Using this estimate, the iteration cycle as in I is started.

In order to show that EBC selects a set of important image pairs in the topology, we initially tested on the graphs whose edges were identified using all-against-all image matching. Edges were ranked according to EBC values and during this computation, edge weights (normalized total number of inliers between image pairs) are used. Edges with EBC score greater than zero were kept to be used in trajectory estimation carried out by minimizing the error in 4. Obtained results are presented in Table II. Average and maximum symmetric transfer errors and standard deviation computed over using all correspondences detected by using all-against-all are given in the table. The computational time required for minimizing the error in 4 are provided in the last column. The minimization was carried out using MATLAB on a personal computer with a 4.00GHz Intel Core i7 processor and 64GB RAM. The approach provided a similar quality of trajectory estimate compared to the ones obtained with using all edges. Time-saving is significantly higher in the denser datasets. For Datasets III and V, the approach in [6] (Table 1) provided similar trajectory accuracy using $2,419$ and $2,719$ overlapping image pairs. When these numbers are compared to the corresponding ones in Table II, 400 lower for the Dataset III and $1,469$ more for the Dataset V. This yields that EBC performed better on the denser dataset compared to the approach in [6]. We also tested the whole framework mentioned throughout this paper using weighted ranking (as in Eq. 1) criterion with two different weight combination ($w_1 = 0.75, w_2 = 0.25$ and $w_1 = w_2 = 0.5$) and graph energy (as in Eq. 2) in the stopping criterion. If the relative change on graph energy is less than $\%25$ in two consecutive iterations, we stopped iterating and continued to the image blending step. Experimental results were compared with the traditional approach of attempting to match all image pairs in the possible overlapping image pair list and updating trajectory estimate [19]. Obtained results are given in Table III. Error measures were computed over all overlapping image pairs identified using all-against-all matching. Successful pairs represent the overlapping image pairs that at least 20 inlier correspondences were detected after outlier rejection while unsuccessful image pairs column represents the total number of image pairs that were attempted to be matched but failed to have at least 20 inliers. From the table, it can be seen that the proposed method was capable of reducing the

TABLE I

MAIN CHARACTERISTICS OF DATA SETS.

Dataset	Image Size	Color	Ratio x100	Total Number of	
				Images	Correspondences
Dataset I	960×540	RGB	4.65	233	$132,999$
Dataset II	1344×752	RGB	1.36	413	$236,725$
Dataset III	512×384	RGB	0.60	$1,136$	$628,859$
Dataset IV	696×520	Grayscale	15.80	142	$395,541$
Dataset V	384×288	Grayscale	5.87	430	$930,898$
Dataset VI	512×384	RGB	11.96	555	$7,992,010$
Dataset VII	384×287	RGB	10.31	268	$1,425,402$

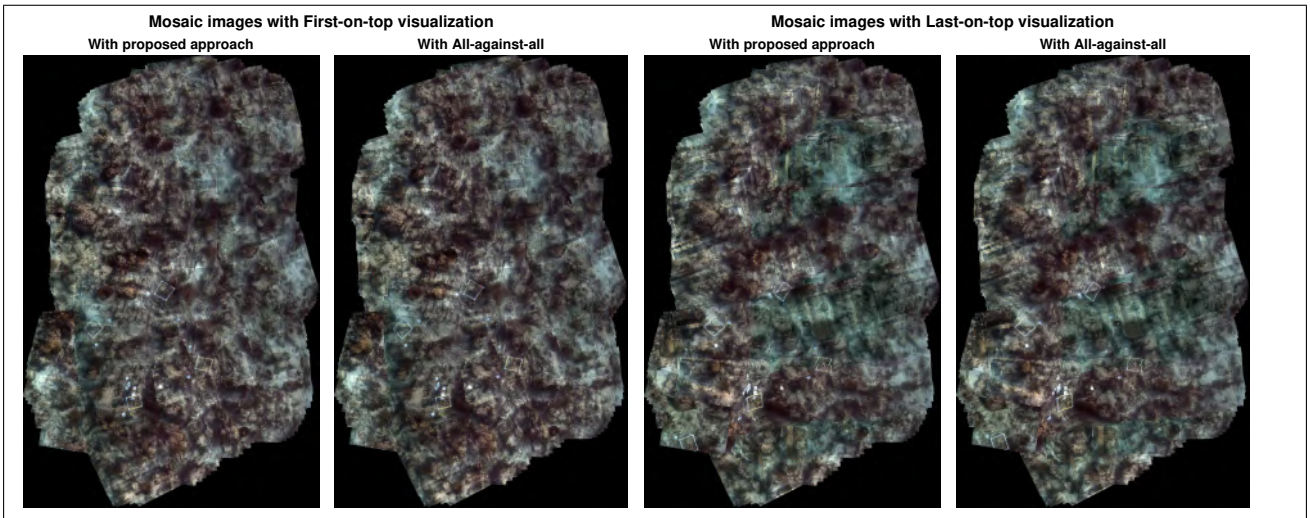

Fig. 3. Mosaic images of Dataset III with two different visualizations. Mosaic images are composed of 1136 images obtained during a survey of coral reef mapping located in the Florida Reef Tract [18]. They are approximately 3600×2400 pixels and 200 pixels per meter.

TABLE II

SUMMARY OF THE OBTAINED RESULTS WITH EBC FILTERED.

Dataset	Method	Total Number of Edges	Average Error (in pix.)	Standard Deviation (in pix.)	Maximum Error (in pix)	Total Time[1](in sec.)
Dataset I	EBC filtered	618	5,81	2.15	48.36	8.12
	All-against-all	1,258	5.55	2.36	52.42	14.68
Dataset II	EBC Filtered	944	21.19	9.80	150.90	28.27
	All-against-all	1,153	20,32	8.86	152.23	35.22
Dataset III	EBC Filtered	2,816	5.88	2.52	41.17	129.15
	All-against-all	3,895	5.59	2.42	42.14	159.44
Dataset IV	EBC Filtered	401	9.45	4.22	59.42	10.42
	All-against-all	1,582	8.97	4.03	53.54	38.13
Dataset V	EBC Filtered	1,250	6.54	2.89	59.86	43.22
	All-against-all	5,412	5.80	2.54	61.08	247.26
Dataset VI	EBC Filtered	2,285	8.94	3.86	48.97	364.50
	All-against-all	18,392	7.11	3.05	32.20	4,423.22
Dataset VII	EBC Filtered	1,182	2.62	0.98	17.22	82.66
	All-against-all	3,688	2.35	0.90	17.13	310.37

total number of overlapping image pairs without sacrificing the final quality of the trajectory accuracy. This provides a substantial amount of time-saving as it does reduce the total number of image matching attempts. Using graph energy as a decision step (Step 5 in Fig. I) removes the necessity of a covariance matrix of the motion parameters as it is used to

TABLE III

SUMMARY OF RESULTS OBTAINED USING PROPOSED METHOD DURING THE TOPOLOGY ESTIMATION PROCESS.

Dataset	Strategy	Successful Pairs	Unsuccessful Pairs	Avg. Error	Std. Deviation	Max. Error
				in pixels		
Dataset I	EBC Filtered $w_1 > w_2$	867	285	5.69	2.51	48.17
	EBC Filtered $w_1 = w_2$	784	198	5.94	6.02	413.23
	The approach in [19]	1,258	3,923	5.55	2.36	52.42
Dataset II	EBC Filtered $w_1 > w_2$	710	571	24.60	43.78	1,528.45
	EBC Filtered $w_1 = w_2$	646	431	25.35	44.86	1,459.56
	The approach in [19]	1,102	2,313	23.52	43.91	1,888.62
Dataset III	EBC Filtered $w_1 > w_2$	2,250	2,117	6.05	3.50	84.04
	EBC Filtered $w_1 = w_2$	2,250	2,114	5.99	3.38	84.92
	The approach in [19]	3,892	45,545	5.59	2.41	42.14
Dataset IV	EBC Filtered $w_1 > w_2$	716	0	9.08	4.09	50.38
	EBC Filtered $w_1 = w_2$	643	16	9.10	4.10	49.53
	The approach in [19]	1,581	238	8.97	4.03	53.54
Dataset V	EBC Filtered $w_1 > w_2$	2,149	5	6.73	6.68	116.65
	EBC Filtered $w_1 = w_2$	2,127	24	6.75	6.74	118.60
	The approach in [19]	5,412	3,712	5.80	2.54	61.08
Dataset VI	EBC Filtered $w_1 > w_2$	3,091	0	7.49	3.46	35.83
	EBC Filtered $w_1 = w_2$	3,072	2	7.50	3.45	36.92
	The approach in [19]	14,862	135	7.10	3.07	34.01
Dataset VII	EBC Filtered $w_1 > w_2$	830	233	2.56	1.05	17.04
	EBC Filtered $w_1 = w_2$	831	204	2.55	1.03	17.16
	The approach in [19]	2,914	528	2.36	0.92	17.11

compute information measure in [10]. This also reduces the need for computational memory and time. On the other hand, the covariance of motion parameters is used in generating possible overlapping image pairs. Not having uncertainty on image positions during the Step 1 list generation caused some inaccuracies in the form of having more image pairs identified as potentially matching. This might cause a slight increase in the total number of image matching attempts made during the process. Also, the selected threshold for image pair to decide whether potentially overlapping or not has also an important role in the total number of image matching attempts. We used a single value for all the datasets tested however, some datasets are much sparser comparing to some other ones. It can be concluded from the Table III that the threshold value used in the experiments was not suitable for Dataset II as even the traditional approach failed. Different weight-set provided similar trajectories except for Dataset I. The failure for that dataset is at some point depends on the trajectory and also related to the stopping criterion. For Dataset III, although the same number of overlapping image pairs were used, the error measures are different. This is due to the overlapping image pairs used were different. The discrepancy between maximum errors for Dataset III and V are relatively large comparing to the other tested datasets. Obtained mosaic images with all-against-all matching and EBC filtered with $w_1 > w_2$ for Datasets III and V are illustrated in Figs. 3 and 4. Despite the discrepancy on a maximum error on trajectory, there is no visually disturbing error on mosaic images.

IV. CONCLUSIONS AND FUTURE WORK

Creating visual maps has become of interest to the science community as the optical data gathering platforms have been advanced lately. Low-cost platforms carrying a camera as the main sensor are usually preferred since they do not require much expertise to use and maintain. Image mosaicing methods have been widely used to create a 2D map of the area surveyed by composing relatively smaller images into a single bigger image. In the absence of any other data, images are the only information source. As the image matching attempts grow in quadratic form, It is desired to obtain the trajectory estimate and the topology (trajectory and overlapping image pairs) with minimum image matching attempts. Previous studies [6], [9] showed that identifying all the overlapping image pairs was not needed to obtain globally coherent image mosaics. In this study, we proposed a method using EBC to rank edges and choose a subset of them to obtain a mosaic image. We presented experimental results with seven different datasets. Experimental results showed that EBC could be used in observation ranking and selection process in processes such as SLAM and image mosaicing. EBC and similarly Node Betweenness Centrality (NBC) could be further used to prune not only the edges but also the nodes in the graph. Also, we noted that graph energy increases smoothly with respect to the total number of edges and this allows for using it as a stopping criterion. Graph energy is advantageous comparing to information measure used in [10] as there is no need to propagate covariance matrix. As future work, we investigate to model the change on graph energy theoretically in the case of adding or deleting some edges and their relation to image mosaicing methods. We also study further on the minimum number of edges to get the globally coherent mosaic.

ACKNOWLEDGMENT

Authors would like to thank Underwater Vision Lab. of University of Girona for providing datasets used in experiments.

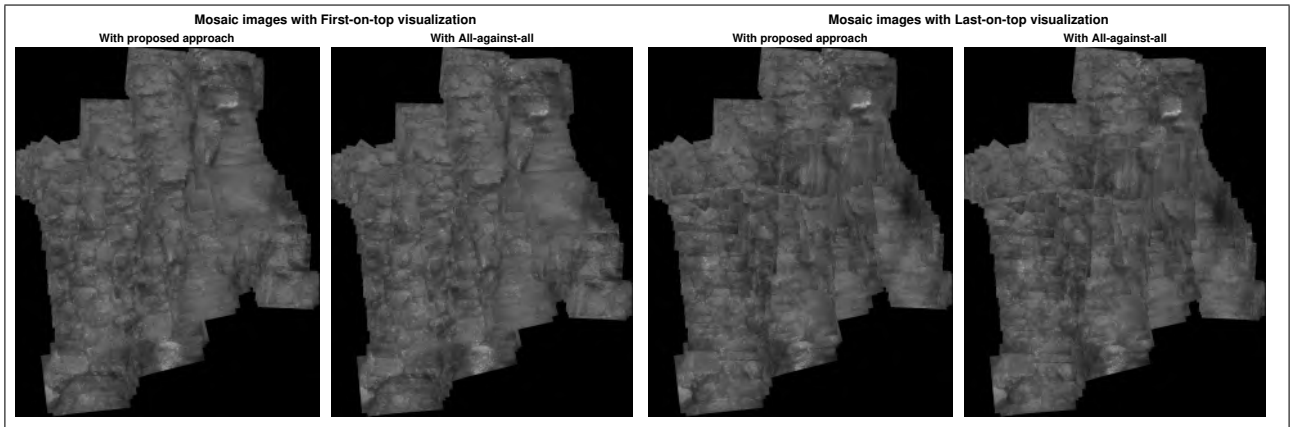

Fig. 4. Mosaic images of Dataset V with two different visualizations. Mosaic images are composed of 430 images obtained during the sea trials of ICTINEU AUV [20]. They are approximately 3400×2800 pixels and 100 pixels per meter

REFERENCES

[1] R. Szeliski, "Image alignment and stitching: A tutorial," *Foundations and Trends® in Computer Graphics and Vision*, vol. 2, no. 1, pp. 1–104, 2006.

[2] S. Hsu, H. S. Sawhney, and R. Kumar, "Automated mosaics via topology inference," *IEEE Computer Graphics and Applications*, no. 2, pp. 44–54, 2002.

[3] B. Triggs, P. F. McLauchlan, R. I. Hartley, and A. W. Fitzgibbon, "Bundle adjustment — a modern synthesis," in *Vision Algorithms: Theory and Practice*, B. Triggs, A. Zisserman, and R. Szeliski, Eds. Berlin, Heidelberg: Springer Berlin Heidelberg, 2000, pp. 298–372.

[4] M. I. A. Lourakis, "Sparse non-linear least squares optimization for geometric vision," in *Computer Vision – ECCV 2010*, K. Daniilidis, P. Maragos, and N. Paragios, Eds. Berlin, Heidelberg: Springer Berlin Heidelberg, 2010, pp. 43–56.

[5] S. Agarwal, K. Mierle, and Others, "Ceres solver," http://ceres-solver.org.

[6] A. Elibol, N. Gracias, R. Garcia, and J. Kim, "Graph theory approach for match reduction in image mosaicing," *J. Opt. Soc. Am. A*, vol. 31, no. 4, pp. 773–782, Apr 2014.

[7] V. Ila, J. M. Porta, and J. Andrade-Cetto, "Information-based compact pose slam," *IEEE Transactions on Robotics*, vol. 26, no. 1, pp. 78–93, 2010.

[8] E. Garcia-Fidalgo, A. Ortiz, F. Bonnin-Pascual, and J. P. Company, "Fast image mosaicing using incremental bags of binary words," in *2016 IEEE International Conference on Robotics and Automation (ICRA)*, May 2016, pp. 1174–1180.

[9] A. Elibol and H. Shim, "Developing a visual stopping criterion for image mosaicing using invariant color histograms," in *Advances in Multimedia Information Processing – PCM 2015*. Cham: Springer International Publishing, 2015, pp. 350–359.

[10] A. Elibol, N. Gracias, and R. Garcia, "Fast topology estimation for image mosaicing using adaptive information thresholding," *Robotics and Autonomous Systems*, vol. 61, no. 2, pp. 125 – 136, 2013.

[11] G. Bounova and O. de Weck, "Overview of metrics and their correlation patterns for multiple-metric topology analysis on heterogeneous graph ensembles," *Phys. Rev. E*, vol. 85, p. 016117, Jan 2012.

[12] M. E. J. Newman and M. Girvan, "Finding and evaluating community structure in networks," *Phys. Rev. E*, vol. 69, p. 026113, Feb 2004.

[13] J. Canny, "A computational approach to edge detection," *IEEE Transactions on pattern analysis and machine intelligence*, no. 6, pp. 679–698, 1986.

[14] I. Gutman, "The energy of a graph: old and new results," in *Algebraic combinatorics and applications*. Springer, 2001, pp. 196–211.

[15] D. Lowe, "Distinctive image features from scale-invariant keypoints," *International Journal of Computer Vision*, vol. 60, no. 2, pp. 91–110, 2004.

[16] M. A. Fischler and R. C. Bolles, "Random sample consensus: a paradigm for model fitting with applications to image analysis and automated cartography," *Communications of the ACM*, vol. 24, no. 6, pp. 381–395, 1981.

[17] R. A. Brualdi, "Energy of a graph," in *Notes for AIM Workshop On Spectra of families of matrices described by graphs, digraphs, and sign patterns*, 2006.

[18] D. Lirman, N. R. Gracias, B. E. Gintert, A. C. R. Gleason, R. P. Reid, S. Negahdaripour, and P. Kramer, "Development and application of a video-mosaic survey technology to document the status of coral reef communities," *Environmental monitoring and assessment*, vol. 125, no. 1-3, pp. 59–73, 2007.

[19] N. R. Gracias, S. Van Der Zwaan, A. Bernardino, and J. Santos-Victor, "Mosaic-based navigation for autonomous underwater vehicles," *IEEE Journal of Oceanic Engineering*, vol. 28, no. 4, pp. 609–624, 2003.

[20] D. Ribas, N. Palomeras, P. Ridao, M. Carreras, and E. Hernandez, "Ictineu AUV wins the first SAUC-E competition," in *IEEE International Conference on Robotics and Automation*, Roma, Italy, April 2007.